Influence of Thermal History on the Nonisothermal Crystallization of Poly(L-lactide)

R. Masirek,[1] E. Piorkowska,[1] A. Galeski,[1] M. Mucha[2]

[1]*Centre of Molecular and Macromolecular Studies, Polish Academy of Sciences, 90 363 Lodz, Sienkiewicza 112, Poland*
[2]*Faculty of Process and Environmental Engineering, Lodz Technical University, 90 924 Lodz, Wolczanska 215, Poland*

Received 7 August 2006; accepted 8 September 2006
DOI 10.1002/app.26047
Published online in Wiley InterScience (www.interscience.wiley.com).

ABSTRACT: The effect of thermal history on the nonisothermal crystallization of poly(L-lactide) (PLA) was studied. The cold crystallization of PLA by heating from the glassy state was dominated by the heating rate. However, the temperature to which PLA was cooled before crystallization markedly affected the crystallization kinetics. The lower the temperature was to which PLA was cooled, the lower the nonisothermal crystallization peak temperature was and the larger the crystallization enthalpy was, which indicated enhanced nucleation of spherulites. Fast heating from the glassy state reduced the time available for the growth of spherulites and also suppressed the number of nuclei stable at elevated temperatures by limiting the recrystallization of nuclei formed at low temperatures and their overgrowth by thicker and more perfect crystals. © 2007 Wiley Periodicals, Inc. J Appl Polym Sci 105: 282–290, 2007

Key words: crystallization; nucleation

INTRODUCTION

Polymer crystallization from the molten state usually begins from heterogeneous nuclei. Homogeneous nucleation becomes active at high undercooling, which is difficult to reach for most crystallizing polymers before the completion of polymer crystallization from heterogeneous nuclei. Such conditions can be sometimes achieved during very fast quenching of thin films and also in polymer droplets that are sufficiently small to be free from any impurities.[1,2]

However, high undercooling is easily accessible in slowly crystallizing polylactide (PLA). Optically pure poly (L-lactide) and poly(D-lactide) are crystallizable polymers. Chiral centers in their structure allow one to vary the enantiomeric compositions of the polylactides. Dimers of different chirality in the PLA chain reduce its ability to crystallize; beyond a certain concentration of the minor comonomer, crystallization does not occur.[3] Slowly crystallizing PLAs can be quenched below their glass-transition temperature (T_g) without noticeable crystallization and then crystallized during subsequent heating.[4] Different crystallinity levels can be reached depending on the molecular architecture and thermal history.[3,5]

Pluta and Galeski[4] demonstrated that different spherulitic patterns emerge during the isothermal crystallization of PLA depending on its thermal history. Spherulite nucleation is greatly enhanced by the cooling of PLA to the glassy state and subsequent heating to the crystallization temperature, instead of direct cooling to the crystallization temperature.

Hernandez Sanchez et al.[6] showed that the number of nuclei can be significantly increased by the annealing of PLA just above the glass transition (73°C) for more than 3 h, which is reflected in its overall crystallization kinetics. Annealing PLA just below T_g (53°C) enhanced the conversion of melt into spherulites; however, the number of nuclei found by atomic force microscopy seemed to be much greater than that expected from the crystallization kinetics.

All these observations led to the conclusion that a significant part of crystallization nuclei appear at lower temperatures above the glass transition. It has become evident that nucleation is time- and temperature-dependent phenomenon. However, because nucleation is not followed immediately by the crystallization of PLA, the nuclei are formed during cooling and are ready to initiate the crystal growth when conditions facilitate the growth. Neither nucleation near T_g nor its impact on the cold crystallization of PLA have been systematically investigated. The aim of this study was to examine the effect of cooling on nucleation and the enhancement of crystallization kinetics. PLA crystallization was studied by means of differential scanning calorimetry (DSC) and light microscopy, whereas spherulite size was characterized by the small-angle light scattering (SALS) method.

This article is dedicated to the memory of Professor Marian Kryszewski.

Correspondence to: R. Masirek (masirek@bilbo.cbmm.lodz.pl).

Journal of Applied Polymer Science, Vol. 105, 282–290 (2007)

TABLE I
Calorimetric Data for PLA Samples of Series A Cooled (First Cooling) from 180°C to Room Temperature and Heated (Second Heating) at Various Rates

Sample code	Cooling rate (K/min)	Heating rate (K/min)	T_c (°C)	ΔH_c (J/g)	T_m (°C)	ΔH_m (J/g)
A-1/1	1	1	104.2[a]	27.3[a]		
			92.6	1.6	150.3, 157.8	30.0
A-5/1	5	1	96.2	29.2	147.7, 157.2	30.7
A-10/1	10	1	97.1	29.1	147.8, 157.2	30.1
A-q/1	Quench	1	96.2	29.4	147.7, 157.1	30.8
A-5/5	5	5	111.3	30.4	149.4, 155.4	31.5
A-10/5	10	5	115.3	31.6	150.2, 155.7	31.7
A-20/5	20	5	114.4	31.6	150.2, 155.3	31.2
A-q/5	Quench	5	116.9	31.7	150.4, 155.4	31.4
A-5/10	5	10	121.2	24.9	151.2	26.5
A-10/10	10	10	122.6	25.4	151.9	26.5
A-q/10	Quench	10	121.2	24.5	151.7	25.4
A-5/20	5	20	132.3	3.0	154.7	3.8
A-20/20	20	20	132.3	3.6	154.0	3.3
A-q/20	Quench	20	132.5	3.3	154.6	3.5
A-20/30	20	30	135.8	0.6	154.6	0.6
A-20/50	20	50	—	—	—	—

[a] Crystallization during cooling.

EXPERIMENTAL

In this study, we used PLA manufactured by Cargill-Dow, Inc. Minnetonka, MN (D-lactide content = 4.1%, residual lactide content = 0.1%). The weight-average molecular weight (M_w) and M_w/number-average molecular weight determined by a size exclusion chromatography in methylene chloride were 126 kg/mol and 1.48, respectively.

Pellets of PLA were vacuum-dried at 100°C for 4 h and then homogenized in a Brabender (Duisburg, Germany) mixer at 190°C for 20 min at 60 rpm under a flow of dry gaseous nitrogen. Ultranox 626 (0.3%) was added to PLA as a stabilizer. After processing, the polymer was stored in a dry atmosphere in a desiccator.

DSC was carried out with a TA Instruments (New Castle, DE) DSC 2920 on specimens weighing 4–4.5 mg. The specimens were heated at the rate of 100 K/min to 180°C, annealed for 3 min, and then subjected to thermal treatment composed of cooling and heating runs at programmed rates and also isothermal annealing at selected temperatures. Dry gaseous nitrogen was purged through the cell during all measurements and thermal treatments. For more efficient cooling, the standard DSC cover was replaced by another, specially designed, cap. It was composed of a thermally insulated aluminum element having the shape of the letter H. To the upper cup of the H, the liquid N_2 was poured, whereas the lower cup covered both the sample and the DSC furnace. The DSC apparatus was able to maintain the control over the cooling rate up to 40 K/min. For faster quenching, the maximum level of LN_2 was kept in the aluminum cup, and the DSC heater was inactive; which allowed the cooling rate to reach 70 K/min. Thermally modulated differential scanning calorimetry (MDSC; TA Instruments 2920) was also used in the studies. Samples cooled from the molten state at various rates were then heated in a modulated differential scanning calorimeter at a rate of 1 K/min, an amplitude of 0.106 K, and a frequency of 1/40 Hz.

Several series of samples were prepared with various cooling and heating conditions. Tables I, II and III contain sample codes, details of thermal treatments and calorimetric data: crystallization peak temperature (T_c), crystallization enthalpy (ΔH_c), melting peak temperature (T_m) and melting enthalpy (ΔH_c).

Samples of series A were cooled to room temperature, which was below the T_g of 57°C, and subsequently heated to 180°C (Table I). The sample codes and the cooling and heating rates are listed in Table I. Both the cooling and heating rates were varied over a wide range.

B1 samples were cooled at 20 K/min to a predetermined target temperature in the range of 70–90°C, annealed there for 10 or 20 min, then cooled to room temperature at the same rate, and subsequently heated at 20 K/min. B2 samples were cooled at 20 K/min to room temperature, heated at 20 K/min to a selected temperature in the range of 70–90°C, annealed there for 10 or 20 min, and heated at 20 K/min to melting. The times and temperatures of the isothermal annealing of the B1 and B2 samples are listed together with sample codes in Table II. Those two sets of experiments were designed to study the effect of annealing time and temperature on crystallization.

TABLE II
Calorimetric Data for PLA Samples of Series B Cooled (First Cooling) from 180°C to Room Temperature and Heated (Second Heating) at 20 K/min with Either Cooling (B1) or Heating (B2) Interrupted by Isothermal Annealing

Sample code	Annealing temperature (°C)	Annealing time (min)	T_c (°C)	ΔH_c (J/g)	T_m (°C)	ΔH_m (J/g)
B1-70/20	70	20	134.3	2.9	154.7	2.9
B1-80/20	80	20	133.8	2.9	153.8	3.1
B1-90/10	90	10	133.3	2.4	152.5	2.8
B2-70/20	70	20	132.6	4.1	153.6	4.8
B2-80/20	80	20	130.2	6.2	152.6	7.5
B2-90/10	90	10	119.6	17.7	152.2	21.4

Samples from the C1 series were cooled at 20 K/min to a selected target temperature in the range of 60–90°C and, after 1 min of nuclei incubation, were heated at a rate of 5 K/min to 180°C The samples from series C2 were cooled to a temperature in the range of 60–80°C and, after 1 min, were heated at 20 K/min to 95°C and then at 5 K/min to 180°C. The codes and conditions of thermal treatment of the C1 and C2 samples are listed in Table III. Experiments with the C1 and C2 samples were aimed at the determination of the nucleation incubation temperature effect on the nonisothermal crystallization during heating.

Samples from the D series were cooled from the molten state to room temperature at 20 K/min, heated at various rates in the range of 30–70 K/min to about 132–133°C, and then cooled again to room temperature at 5 K/min.

Polarized light microscopy was applied to directly observe the crystallization of PLA during selected thermal treatments. Thin films 50 μm thick were obtained by compression molding between cover microscope slides at 180°C followed by quenching to room temperature. These films were heated to 180°C, annealed there for 3 min, and then subjected to thermal treatment composed of cooling and heating runs at programmed rates under a flow of dry gaseous nitrogen in a Linkam THMS600 (Waterfield, UK) hot stage mounted in a polarized light microscope and equipped with a TMS92 control unit. The crystallization of the samples was monitored by polarized light microscopy and a video camera connected to a video recorder and a PC with a frame grabber card. The average spherulite radius in the crystallized films subjected to the selected thermal treatment in the hot stage was measured by a SALS method. The SALS studies used a He–Ne laser as a light source with a wavelength of 0.6328 μm. Scattering patterns were recorded photographically. The light intensity distribution versus the scattering angle was determined at an azimuthal angle of 45°C and it was used for the calculation of average radius according to the method described in detail in ref. 7.

The temperature dependence of the growth rate of PLA spherulites was measured during the isothermal crystallization of 10 μm thick films by polarized light microscopy in the Linkam hot stage at various crystallization temperatures. The films prepared in the same way as the thicker films for observations of crystallization were melt-annealed at 180°C for 3 min and then cooled to a predetermined temperature to crystallize isothermally. Several samples were examined at each crystallization temperature, and the average value of the spherulite growth rate was calculated.

TABLE III
Calorimetric Data for PLA Samples of Series C1 Cooled at 20 K/min from 180°C to the Target Temperature of 60–90°C and Heated (Second Heating) at 5 K/min and for Samples of Series C2 that Were Cooled at 20 K/min to the Target Temperature of 60–80°C and Heated (Second Heating) at 20 K/min to 95°C and at 5 K/min to Melting

Sample code	Target temperature (°C)	T_c (°C)	ΔH_c (J/g)	T_m (°C)	ΔH_m (J/g)
C1-60	60	118.0	27.7	150.8	28.1
C1-65	65	122.0	22.8	152.0	22.7
C1-70	70	124.1	19.6	152.3	20.1
C1-90	90	128.7	7.4	153.2	7.8
C2-60	60	119.6	25.8	151.6	25.5
C2-65	65	121.9	21.8	152.2	22.3
C2-70	70	125.8	15.6	152.8	15.6
C2-80	80	128.7	8.2	153.1	8.2

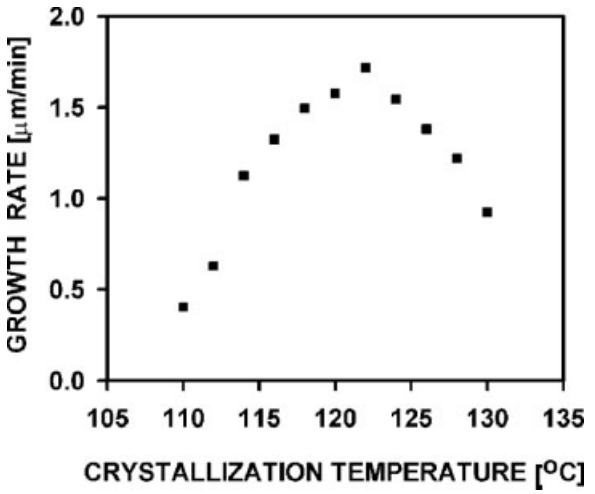

Figure 1 Dependence of PLA spherulite growth rate on crystallization temperature.

RESULTS

The temperature dependence of the spherulite growth rate of PLA studied is shown in Figure 1. The growth rate increased with decreasing temperature, passed through a maximum at about 122°C, and then decreased in a fashion similar to that observed in ref. 8. However, the largest value, 1.7 μm/min, was lower than the maximum value measured in ref. 8 for PLA with a similar M_w of 200,000 g/mol, which was about 3 μm/min, because of a higher content of D-lactide (4.1%) in our samples.

Calorimetric data for the samples of series A are collected in Table I. Figure 2 demonstrates the exemplary DSC thermograms of PLA. The samples were recorded during cooling to the glassy state at various rates and during subsequent heating at 1 K/min.

On the DSC thermogram recorded during cooling at 1 K/min, flat and broad crystallization exotherm appeared centered around 104°C and was associated with a crystallization enthalpy of 27 J/g. Only a small and rather flat exotherm was discernible on the second heating thermogram at about 93°C, whereas at higher temperatures, two melting peaks appeared, the lower at 150°C and the higher at 158°C, associated with a total melting enthalpy of 30 J/g.

The DSC thermogram recorded during the cooling of PLA at a rate of 5 K/min did not exhibit a crystallization exotherm. Neither crystallization was observed during cooling at higher rates. The heating thermograms, recorded during the second heating, exhibited crystallization peaks around 96–97°C and two melting peaks, the lower around 148°C and the higher around 157°C. The melting enthalpy of 30–31 J/g, corresponding well to the crystallization enthalpy, and peak positions were similar for all samples independent of the cooling rate.

Figure 3 shows the exemplary DSC thermograms recorded during faster heating. With increasing heating rate, the cold crystallization peak shifted to higher temperatures; it was centered around 111–117, 121–122, and 132°C for heating at 5, 10, and 20 K/min, respectively. The corresponding crystallization enthalpies were about 31–32, 25–26, and 3–4 J/g, which pointed out that during heating at rates of 10 and 20 K/min, PLA cold crystallization did not complete before the onset of melting. The double melting peaks were observed during heating at the rate of 5 K/min at 150–151 and 155–156°C, whereas at heating rates of 10 and 20 K/min, melting was associated with single peaks around 151–152 and 154–155°C, respectively. The melting enthalpy usually corresponded to the crystallization enthalpy, except for the samples cooled and heated at a rate of 5 K/min, where the melting enthalpy slightly exceeded the cold crystallization enthalpy because of the melting of crystals formed during cooling. An increase in the heating rate to 30 K/min resulted in a very weak crystallization beginning about 115°C and reaching a peak rate at 136°C. Sample A-20/50 did not crystallize upon heating at a heating rate of 50 K/min.

Morphological observations of films with thermal history similar to that of the A samples were performed with polarized light microscopy. During

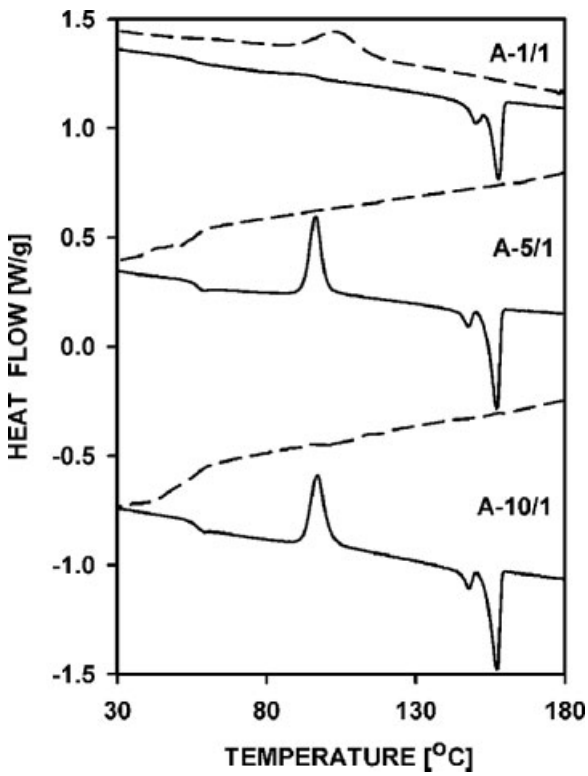

Figure 2 First cooling (dashed line) and second heating (solid line) DSC thermograms of samples A-1/1, A-5/1, and A-10/1. The thermograms shifted vertically.

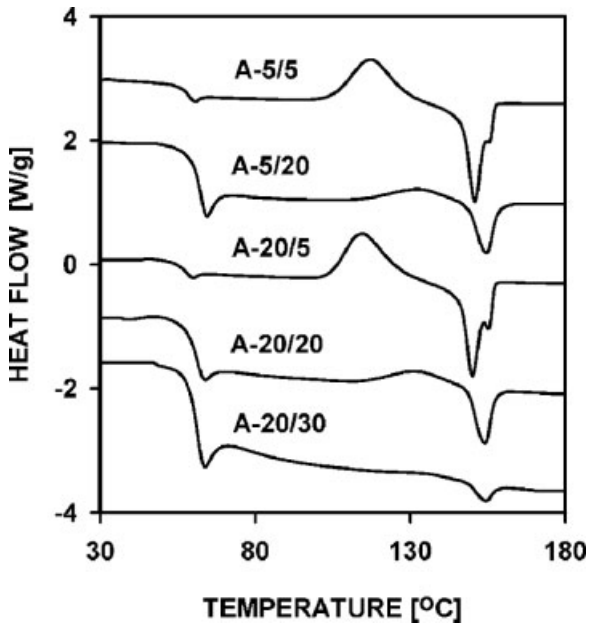

Figure 3 Second heating DSC thermograms of samples A-5/5, A-5/20, A-20/5, A-20/20, and A-20/30. The thermograms shifted vertically.

cooling at 1 K/min in the Linkam hot stage, the first spherulites became discernible around 120°C, which was near the temperature where the crystallization exotherm recorded during the DSC experiment departed from the baseline. As the temperature decreased, new spherulites appeared during further crystallization. The average spherulite radius measured by the SALS method after the sample was cooled to room temperature was 11.2 μm, which corresponded well to spherulite sizes visible under a light microscope, as shown in Figure 4(a). During the cooling of the PLA film in the hot stage at 5 K/min, small spherulites emerged from the amorphous phase at about 110°C, and their number increased with decreasing temperature. They did not enlarge significantly upon cooling to the glassy state [Fig. 4(b)] as the growth rate was very low in this temperature range (cf. Fig. 1). In the samples cooled to room temperature at 10 and 20 K/min [Fig. 4(c)], no spherulites were observed by light microscopy.

During heating from the glassy state at 1 K/min, numerous spherulites appeared in PLA around 90°C. To determine the influence of the cooling history on the average spherulite size in the cold-crystallized samples, the samples were cooled at 5 and 10 K/min, heated subsequently at 1 K/min to 120°C, and quenched down to room temperature. The sample volume was filled with spherulites. The sample cooled at 10 K/min contained only very fine spherulites, as visible in Figure 5(b). On the contrary, the sample cooled at 5 K/min contained a fraction of larger spherulites [Fig. 5(a)] grown during cooling. The sizes of the average spherulites determined by the SALS technique were 5.7 and 4.1 μm for cooling rates of 5 and 10 K/min, respectively.

In the samples heated from the glassy state at 5, 10, and 20 K/min, numerous spherulites appeared at about 100, 110, and 120°C, respectively. The samples cooled at 10 K/min contained only fine spherulites after cold crystallization. In the samples cooled at 5 K/min, there were also spherulites grown during cooling and enlarged during heating that led to a bimodal size spherulite pattern. This is illustrated in Figure 5(c,d), which shows spherulitic patterns in

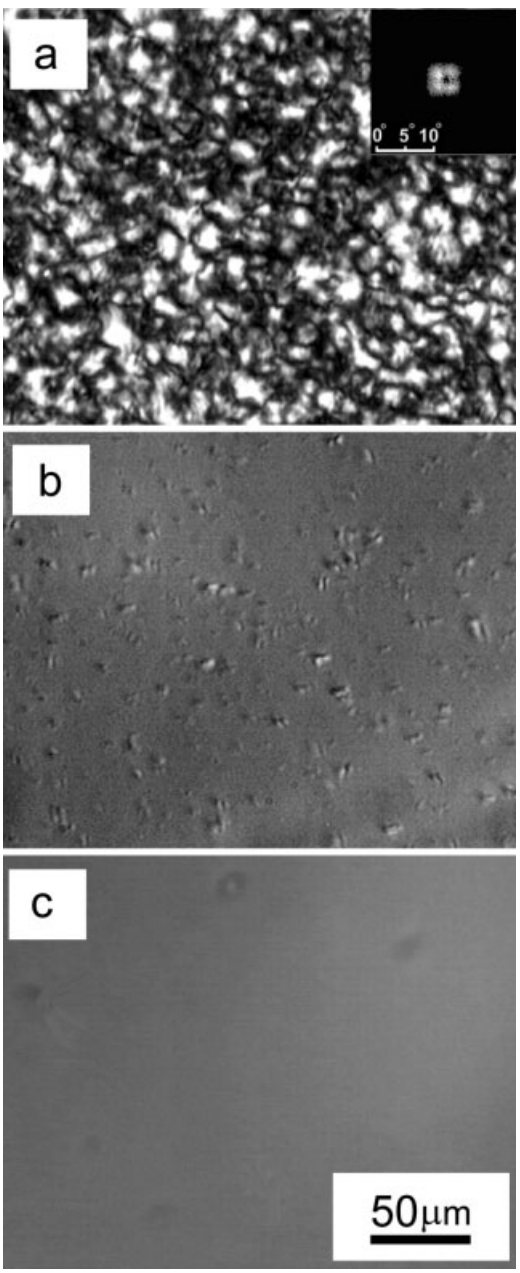

Figure 4 Polarized light micrographs of the PLA films cooled in a Linkam hot stage from 180°C to room temperature at (a) 1, (b) 5, and (c) 10 K/min. The insert in Figure 4(a) shows the SALS pattern.

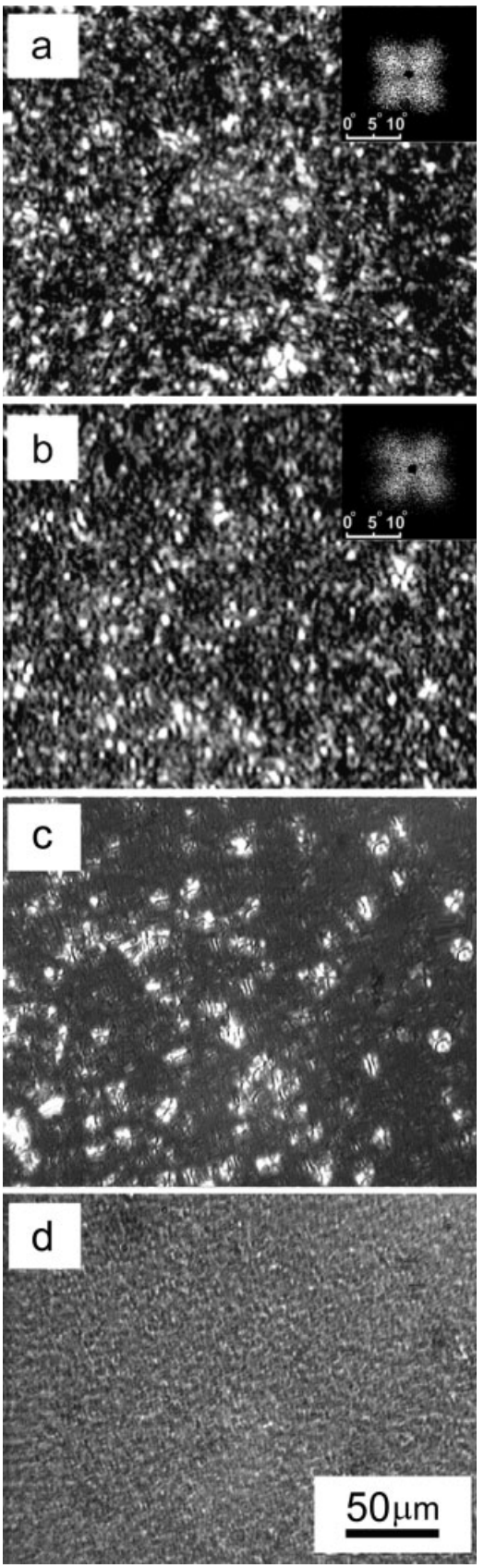

the samples cooled from 180°C to room temperature at 5 K/min [Fig. 5(c)] and 10 K/min [Fig. 5(d)] and heated at 20 K/min to 130°C, where the photographs were taken. During heating at 5 K/min, the crystallization was immediately followed by melting. Therefore, to prepare the samples for the SALS studies, the heating in the hot stage was stopped at 117°C, (close to the DSC crystallization peak temperatures during heating at 5 K/min) at which the samples were annealed for 1 h to complete the crystallization and quenched to room temperature. Despite the different cooling history, the sizes of the average spherulites in the samples cooled at 5 and 10 K/min were similar, about 4.5 μm; the corresponding spherulite patterns are shown in Figure 6(a,b).

The microscope observations indicate very clearly that although the cold crystallization seemed to be dominated by heating rate, cooling history affected the nucleation. A low cooling rate of 1 K/min was sufficient for the complete crystallization of PLA. A cooling rate of 5 K/min resulted in the formation of tiny spherulites visible by light microscopy, although not evidenced by the DSC technique. Surprisingly, subsequent heating (at 10 or 20 K/min) did not reveal a marked difference between the crystallization of samples cooled at 5 K/min [Fig. 4(b)] and 10 K/min [Fig. 4(c)]. Apparently, although not seen under a light microscope, in the sample from Figure 4(c), a significant number of germs were formed during cooling. Calorimetric data for samples from series B1 and B2 are collected in Table II, whereas the exemplary DSC heating scans are shown in Figure 7. The crystallization exotherms of B1-70/20 and B1-90/10 were similar to that of A-20/20, which indicated that the interruption of the cooling by isothermal annealing at 70–90°C for 10 or 20 min had no effect on the subsequent cold crystallization on fast heating at 20 K/min. On the contrary, the isothermal annealing segment introduced during heating effectively lowered the peak crystallization temperature and increased the crystallization enthalpy, as follows from the data in Table II and Figure 7. The effect was augmented by the higher annealing temperature. The melting temperature of the resulting crystals was not significantly affected, whereas the melting enthalpy increased and became larger

Figure 5 Polarized light micrographs of the PLA films cooled and heated in a Linkam hot stage. Films shown in Figure 5(a,b) were cooled from 180°C to room temperature at (a) 5 and (b) 10 K/min and were then heated at 1 K/min to 120°C and quenched to room temperature. Films shown in Figure 5(c,d) were cooled from 180°C to room temperature at (c) 5 and (d) 10 K/min, heated at 20 K/min to 130°C, where the photographs were taken. The inserts in Figure 5(a,b) show the SALS patterns.

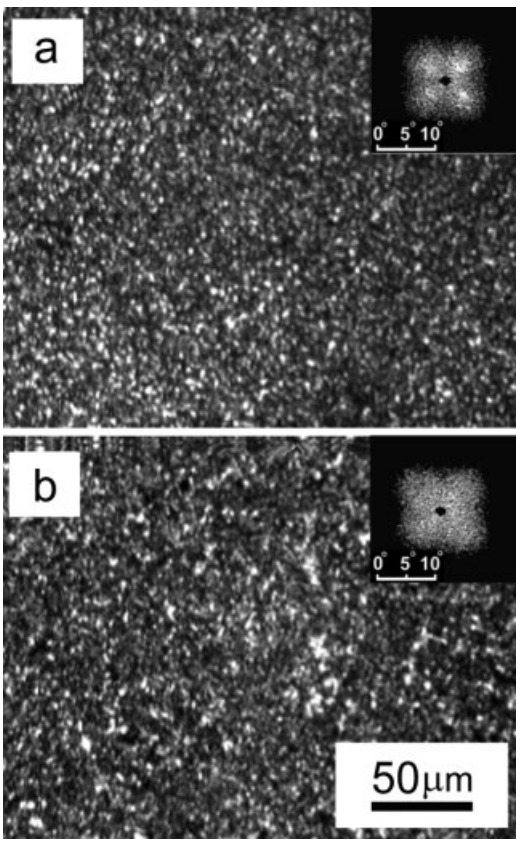

Figure 6 Polarized light micrographs of PLA films after they were cooled from 180°C to room temperature at (a) 5 and (b) 10 K/min and then heated at 5 K/min to 117°C, with annealed at 117°C and quenched to room temperature. The inserts show the SALS patterns.

than the crystallization enthalpy, especially for the sample B2-90/10. Thus, the B2 samples began to crystallize during the annealing steps via the growth of spherulites from nuclei formed during the pre-annealing thermal history that also caused the enhancement of postannealing nonisothermal crystallization.

Figure 8 shows the exemplary thermograms recorded during the second heating of samples from the C1 and C2 series, whereas the calorimetric data are collected in Table III. The decrease of target temperature to which the sample was cooled resulted in lowering of the temperature of the crystallization peak during heating, even by 10 K, and in an increase of the crystallization enthalpy. The melting peak temperatures were affected little, shifting to lower temperatures by 2 K, whereas the melting enthalpy remained equal to the crystallization enthalpy. Obviously, cooling to lower temperatures enhanced the spherulite nucleation. The effect of longer time elapsed at lower temperatures due to longer cooling could be excluded on the basis of the results obtained for the B1 samples. From the comparison of the C1 and C2 samples, it was also clear that the heating rate in temperature below 95°C, had a minor

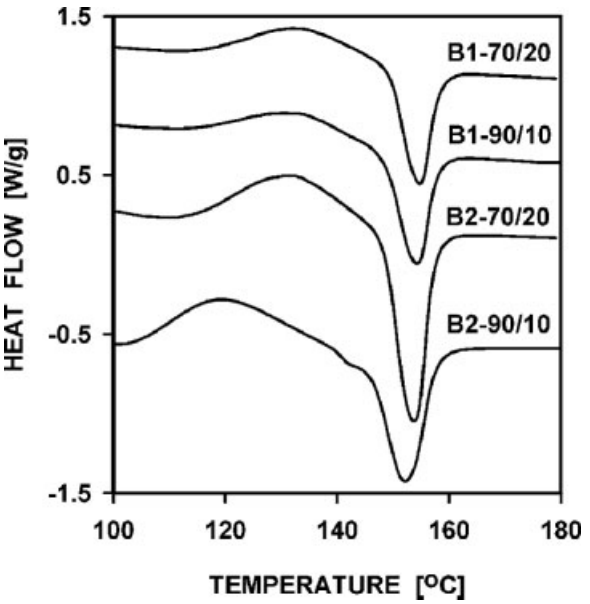

Figure 7 DSC thermograms recorded during second heating of samples B1-70/20, B1-90/10, B2-70/20, and B2-90/10. The thermograms shifted vertically.

effect on cold crystallization. The C1-60 and C2-60 samples crystallized similarly to the samples from series A heated at 5 K/min, with nearly the same crystallization enthalpy and crystallization peak temperature. Thus, passing through the glass transition was not essential for the enhancement of nucleation.

One can expect that the nuclei formed at low temperature were less stable and had lower melting temperatures than those appearing at higher temper-

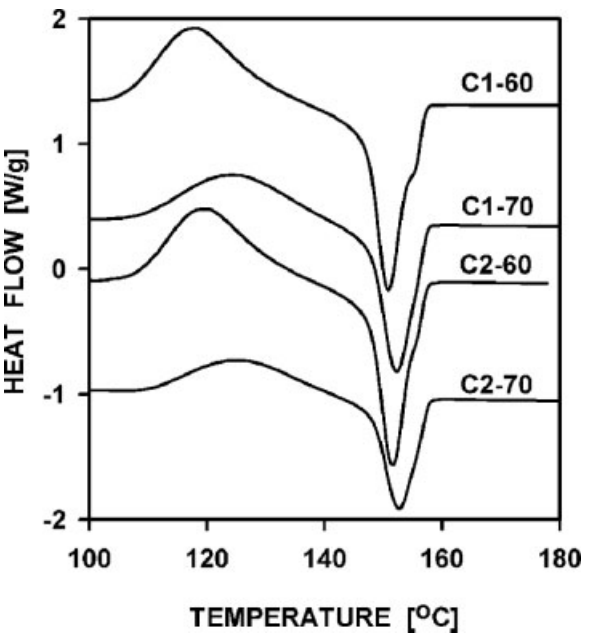

Figure 8 DSC thermograms recorded during second heating of samples C1-60, C1-70, C2-60, and C2-70. The thermograms shifted vertically.

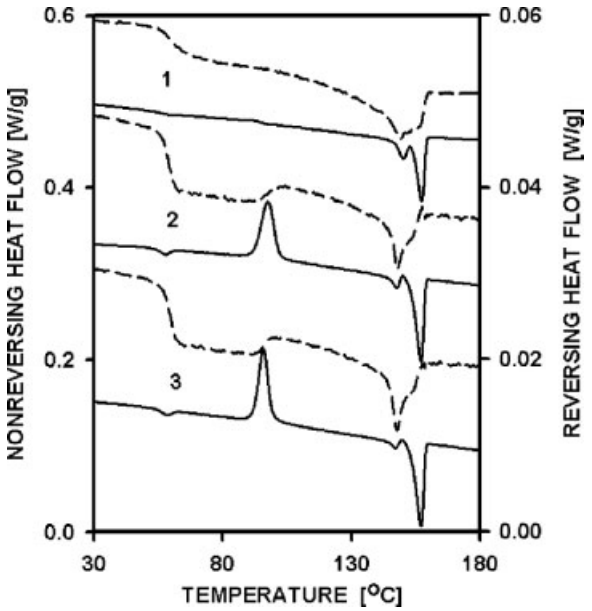

Figure 9 MDSC thermograms recorded during the heating of samples cooled to room temperature at (1) 1, (2) 5, and (3) 10 K/min; the dashed line indicates reversing heat flow, and the solid line indicates nonreversing heat flow. The thermograms shifted vertically.

atures. However, during slow heating, less stable crystals, formed at low temperatures, could recrystallize into crystals having higher melting points. Figure 9 shows MDSC heating thermograms of samples cooled previously from 180°C to room temperature at 1, 5, and 10 K/min. Samples cooled at 5 and 10 K/min crystallized on heating in MDSC, beginning at 90°C in a similar fashion to ordinary DSC. The recrystallization phenomena in those samples, reflected in reversing signal endotherms, began at about 110°C, above the crystallization temperature range, similarly to that seen in ref. 9. During cooling at 1 K/min, crystallization was nearly completed (cf. Fig. 2); therefore, only a small exotherm was discernible in the MDSC nonreversing signal thermogram. The reversing signal departed from the baseline at about 95°C, which indicated the beginning of recrystallization. Spherulites crystallized below 90°C occupied approximately 7 wt % of this sample, as judged from the respective crystallization enthalpy of 2 J/g. Most possibly, this fraction of crystals was less thermally stable and underwent recrystallization in a temperature range lower than that of the other samples studied by the MDSC technique.

Endothermic peaks of the reversing heat flow thermograms in Figure 9 coincided with the low-temperature melting peaks of nonreversing heat flow. This indicated that although a fraction of the crystals melted nonreversibly, another fraction underwent reorganization that increased their melting temperature. Thus, the reorganization of the crystal structure may have contributed to the double melting peaks seen on the thermograms shown in Figures 2 and 3 for samples heated at 1 and 5 K/min; particularly, that a slow heating enabled the crystallization of PLA at relatively low temperatures and also facilitated the recrystallization phenomena.

It is well known that faster heating limits or even eliminates recrystallization phenomena, and therefore, it may decrease the melting temperature of crystals. Fast heating can also hinder the growth of thicker and more thermally stable crystals from nuclei formed at low temperatures below 90°C. Thus, the rate of heating from the glassy state should have influenced the number of nuclei remaining active in PLA at higher temperature. This was illustrated by the crystallization behavior of the samples of the D series heated from the glassy state to about 132–133°C at various rates: 30, 50, and 70 K/min. The target temperature was selected as being still below the melting point of crystals formed at high temperatures during heating at 30 K/min.

The crystallization behavior of the D-series samples demonstrated that a very rapid temperature increase could hinder the crystallization during subsequent cooling, as illustrated in Figure 10. Sample A-20/30 began to crystallize on heating at 115°C, and reached before melting about 2% of crystallinity level that developed in samples heated at 1 or 5 K/min. Therefore, when the heating was stopped at about 133°C and D-30 sample was cooled at 5 K/min, the crystallization continued with a peak temperature at 112°C. Sample A-20/50 did not crystallize on heating from the glassy state. However,

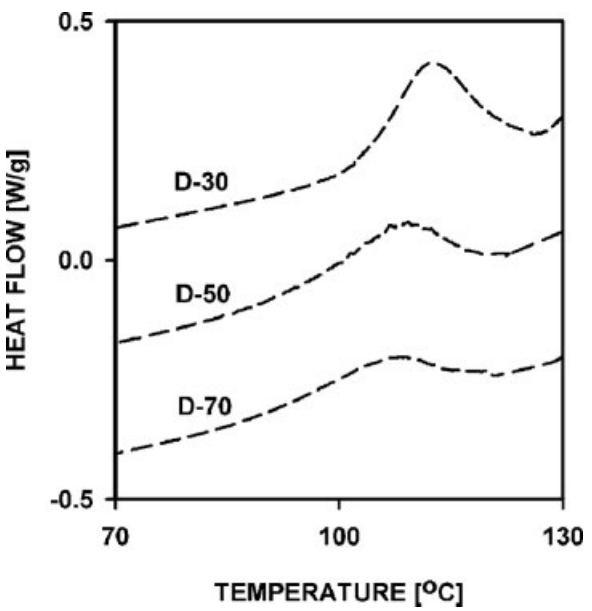

Figure 10 DSC thermograms recorded during the second cooling of D samples heated previously to 130°C at 30 K/min (D-30), 50 K/min (D-50), and 70 K/min (D-70).

when heating was stopped and D-50 sample was cooled, the crystallization exotherm showed up with a peak at 109°C. With the increase of the second heating rate to 70 K/min, the crystallization peak temperature during cooling shifted to 107°C, due to diminished nucleation intensity. The crystallization exotherm decreased and broadened in parallel with the decrease of the crystallization peak temperature; the enthalpy of crystallization also decreased from about 29 J/g for D-30 to 22 J/g for D-50 and 18 J/g for D-70.

CONCLUSIONS

The results obtained indicate that the crystallization of PLA during heating from low temperatures was initiated by nuclei formed during the preceding cooling. The temperature to which the sample was cooled was an important factor; the lower the temperature was, the more enhanced the nucleation and the crystallization upon subsequent heating were. Theory of homogeneous nucleation predicts sporadic formation of nuclei dependent on undercooling. Although the number of heterogeneous nuclei is limited by the number of seeds, new homogeneous nuclei can be formed until the completion of conversion of the melt into spherulites. The enhancement of nucleation in this study was achieved by fast cooling to low temperatures near the T_g. The nucleation process was obviously very quick. In ref. 6, annealing for several hours was necessary to achieve a marked enhancement of nucleation at 53 and at 70°C, despite the high stereoregularity of PLA (reflected, e.g., in its high melting point, ca. 175°C). This raises the question as to whether the phenomena observed in this study were related to the homogeneous process or not.

At low undercoolings, the nucleation of PLA crystallization, although weak, was most probably heterogeneous in nature, as in other crystallizable polymers. As the temperature decreased and the energy barrier of the formation of critical nucleus decreased, the heterogeneous nucleation intensified. Thus, we concluded that the fast nucleation of PLA crystallization, enhanced by large undercooling, was heterogeneous in nature, whereas the real homogeneous process required a much longer time, as shown in ref. 6.

The rate of heating from the glassy state was an important factor influencing the crystallization of PLA, as it is controlled the time available for the growth of spherulites. However, it also influenced the spherulite nucleation. Nuclei formed at high undercooling exhibited low melting temperatures. However, given sufficient time during heating, they recrystallized and/or initiated the growth of other crystals; both mechanisms led to nuclei that were thermally more stable. Fast heating hindered both processes and diminished the number of nuclei remaining active at elevated temperature.

The authors thank Cargill-Dow Polymers, LLC, for supplying PLA and CMMS PAS for supporting the research.

References

1. Koutsky, J. A.; Walton, A. G.; Baer, E. J Appl Phys 1967, 38, 1832.
2. Bernal-Lara, T. E.; Liu, R. Y. F.; Hiltner, A.; Baer, E. Polymer 2005, 46, 3043.
3. Brochu, S.; Prud'homme, R. E.; Barakat, I.; Jerome, R. Macromolecules 1995, 28, 5230.
4. Pluta, M.; Galeski, A. J. Appl Polym Sci 2002, 86, 1386.
5. Migliaresi, C.; De Lollis, A.; Fambri, L.; Cohn, D. Clin Mater 1991, 8, 111.
6. Hernandez Sanchez, F.; Molina Mateo, J.; Romero Colomer, J.; Salmeron Sanchez, M.; Gomez Ribelles, J. L.; Mano, J. F. Biomacromolecules 2005, 6, 3283.
7. Stein R. S.; Rhodes, M. B. J Appl Phys 1960, 31, 1873.
8. Miyata, T.; Masuko, T. Polymer 1998, 39, 5515.
9. Kulinski, Z.; Piorkowska, E. Polymer 2005, 46, 10290.